Annealing studies combined with low temperature emission Mössbauer spectroscopy of short-lived parent isotopes: Determination of local Debye–Waller factors

Gunnlaugsson, H. P.; Masenda, H.; Mølholt, T.E.; Bharuth-Ram, K.; Ólafsson, S.; Johnston, K.; Schell, J.; Gislason, H. P.; Krastev, P. B.; Mantovan, R.

Total number of authors:
13

Published in:
Review of Scientific Instruments

Link to article, DOI:
10.1063/5.0020951

Publication date:
2021

Document Version
Publisher's PDF, also known as Version of record

Review of Scientific Instruments

Annealing studies combined with low temperature emission Mössbauer spectroscopy of short-lived parent isotopes: Determination of local Debye–Waller factors

Cite as: Rev. Sci. Instrum. **92**, 013901 (2021); https://doi.org/10.1063/5.0020951
Submitted: 07 July 2020 . Accepted: 20 December 2020 . Published Online: 08 January 2021

H. P. Gunnlaugsson, H. Masenda, T. E. Mølholt, K. Bharuth-Ram, S. Ólafsson, K. Johnston, J. Schell, H. P. Gislason, P. B. Krastev, R. Mantovan, D. Naidoo, B. Qi, and I. Unzueta

Review of Scientific Instruments ARTICLE scitation.org/journal/rsi

Annealing studies combined with low temperature emission Mössbauer spectroscopy of short-lived parent isotopes: Determination of local Debye–Waller factors

Cite as: Rev. Sci. Instrum. 92, 013901 (2021); doi: 10.1063/5.0020951
Submitted: 7 July 2020 • Accepted: 20 December 2020 •
Published Online: 8 January 2021

H. P. Gunnlaugsson,[1,a)] H. Masenda,[2] T. E. Mølholt,[3] K. Bharuth-Ram,[4,5] S. Ólafsson,[1] K. Johnston,[6] J. Schell,[6,7] H. P. Gislason,[1] P. B. Krastev,[8] R. Mantovan,[9] D. Naidoo,[2] B. Qi,[1] and I. Unzueta[10]

AFFILIATIONS

[1] Science Institute, University of Iceland, Dunhaga 3, IS-107 Reykjavík, Iceland
[2] School of Physics, University of the Witwatersrand, Johannesburg 2050, South Africa
[3] DTU Health Technology, Risø Campus, Frederiksborgvej 399, 4000 Roskilde, Denmark
[4] School of Chemistry and Physics, University of KwaZulu-Natal, Durban 4001, South Africa
[5] Physics Department, Durban University of Technology, Durban 4000, South Africa
[6] EP Department, ISOLDE/CERN, 1211 Geneva 23, Switzerland
[7] Institute for Materials Science and Center for Nanointegration Duisburg-Essen (CENIDE), University of Duisburg-Essen, 45141 Essen, Germany
[8] Institute for Nuclear Research and Nuclear Energy, Bulgarian Academy of Sciences, 72 Tsarigradsko Chaussee Boulevard, Sofia 1784, Bulgaria
[9] CNR-IMM, Unità di Agrate Brianza, Via Olivetti 2, 20864 Agrate Brianza (MB), Italy
[10] Department of Applied Mathematics, University of the Basque Country (UPV/EHU), Torres Quevedo Ingeniaria Plaza 1, 48013 Bilbao, Spain

[a)] **Author to whom correspondence should be addressed:** hpgunnlaugsson@gmail.com

ABSTRACT

An extension of the online implantation chamber used for emission Mössbauer Spectroscopy (eMS) at ISOLDE/CERN that allows for quick removal of samples for offline low temperature studies is briefly described. We demonstrate how online eMS data obtained during implantation at temperatures between 300 K and 650 K of short-lived parent isotopes combined with rapid cooling and offline eMS measurements during the decay of the parent isotope can give detailed information on the binding properties of the Mössbauer probe in the lattice. This approach has been applied to study the properties of Sn impurities in ZnO following implantation of ^{119}In ($T_{\frac{1}{2}}$ = 2.4 min). Sn in the 4+ and 2+ charge states is observed. Above $T > 600$ K, Sn^{2+} is observed and is ascribed to Sn on regular Zn sites, while Sn^{2+} detected at $T < 600$ K is due to Sn in local amorphous regions. A new annealing stage is reported at $T \approx 550$ K, characterized by changes in the Sn^{4+} emission profile, and is attributed to the annihilation of close Frenkel pairs.

INTRODUCTION

An understanding of implantation-induced effects in host materials and their annealing behavior is essential to unravel the physics of damage recovery and open up the possibility of tailoring the electrical, magnetic, and optical properties of materials with appropriate tuning of the doping and annealing.[1]

Over the years, ion implantation has proved to be a key processing step in material modification. Its success stems from the ability to circumvent solubility and diffusion limits compared with other doping techniques. Moreover, ion implantation is an attractive option for material fabrication because nearly all elements can be incorporated in a material with precise control of concentration and depth distribution by varying the fluence and ion beam energy, respectively. More importantly, the combined use of implanted short-lived radioactive isotopes and the sensitivity of emission Mössbauer Spectroscopy (eMS) to minor changes in the nuclear energy levels presents a unique method that is twofold: (i) material modification by introducing the desired dopants to enhance material properties and (ii) characterization at an atomic level using emitted by-products from the decay chain. This provides information on lattice sites of incorporated desired daughter dopants in a crystal, its site changes with materials thermal annealing, and the complexes that the probe ions form.

Several techniques can be utilized to investigate implantation damage on an atomic scale, such as Mössbauer spectroscopy. Of particular importance is emission Mössbauer spectroscopy employing short-lived parent isotopes (^{57}Mn → ^{57}Fe, $T_{\frac{1}{2}}$ = 1.45 min and ^{119}In → ^{119}Sn, $T_{\frac{1}{2}}$ = 2.4 min), as applied by the Mössbauer collaboration at ISOLDE/CERN.[2–4] The method allows for the study of implantation damage at low fluences down to ~10^{11} cm^{-2} (local concentration down to ~10^{-4} at. %) with annealing times dictated by the lifetime of the parent isotope. Furthermore, the low fluences available at ISOLDE ensure that precipitation, clustering, and/or overlapping damage cascades are effectively ruled out.

The resulting Mössbauer spectra provide a wealth of information on the environment of the Mössbauer isotope, such as the charge state, nature, and symmetry of probe sites through the electric quadrupole interaction, magnetic interactions, and binding properties from the Debye–Waller factor.[5] These quantities are sensitive only to the atomic arrangement few lattice atoms away from the probe atom, giving truly local information.

Usually, information on annealing reactions is retrieved from a series of temperature-dependent eMS measurements (*temperature series*), utilizing online measurements where the implantation temperature is the same as the measurement temperature. The general assumption is that at low temperatures, the spectra are dominated by components arising from Fe/Sn in implantation induced amorphous zones that do not anneal during the lifetime of the parent isotope (^{57}Mn/^{119}In) (see, e.g., discussion in Ref. 6). When the implantation and measurement temperature is increased, the intensity of such defect components reduces due to thermally activated annealing, accompanied by a corresponding increase in the intensity of components due to Fe/Sn on regular lattice sites.

There are constraints to how high temperatures can feasibly be applied for temperature series studies in online eMS measurements. The intensity of spectral components is proportional to the Debye–Waller factor, which decreases exponentially with increasing temperature (high temperature approximation). This can result in too low intensity of spectral components to allow for unambiguous interpretation of the spectra. In some cases, interesting physics of the material, such as magnetic interactions, occur at lower temperatures, but implantation at higher temperatures is required in order to anneal the implantation induced damage on the lattice.

Although the implantation damage can impede investigations, there are cases where the study of the physics of these defects is essential, as illustrated, for example, by the results obtained after implantation of ^{57}Mn into rutile TiO_2.[7] The lattice with amorphous regions was found to recover at temperatures below room temperature, and the charge state and properties of the Fe atoms were determined by the type and nature of point defects in the vicinity of the probe atom. Subsequently, from implantations/measurements at different elevated temperatures, it was possible to determine the onset of titanium vacancy mobility at ~330 K and the disassociation of substitutional Mn–oxygen vacancy pairs at ~550 K.[7]

Annealing/implantation at elevated temperatures and measurements at low temperatures is a challenging task when applied to parent isotopes with lifetimes of few minutes. This was, however, first successfully undertaken by Weyer *et al.* in the 1980s using implantation of ^{119}In in Si and Ge.[8,9] These researchers described the annealing of implanted samples for a few minutes, which were then rapidly cooled in liquid nitrogen to perform offline measurements at corresponding temperatures, leaving enough activity in the samples to yield spectra with sufficient statistics. This method was very beneficial in the interpretation of damage components in the spectra and allowed the determination of the isomer-shift and other properties of dilute ^{119}Sn impurities in group IV semiconductors.[8,9]

In this paper, we describe the use of a new apparatus for facilitating rapid cooling experiments using short-lived parent isotopes. The determination of how the binding properties of the probe atom (through the Debye temperature at the probe site) can be retrieved from such measurements is discussed. The technique is applied in the study of ^{119}In implanted ZnO. It is demonstrated that the method yields additional information on the properties of the implantation damage in ZnO in comparison with the analysis of eMS data obtained in a regular temperature series of measurements.[6]

Our earlier studies on temperature series data obtained after implantation of ^{119}In into commercial hexagonal ZnO single crystals were reported by Mølholt *et al.*[6] The results revealed that the implantation process creates acceptor defects that stabilize the Sn^{4+} state rather than Sn^{2+}. The Sn^{2+} state was observed at temperatures below 400 K, most likely due to implantation damage; it showed a considerable increase in area fraction between 600 K and 700 K due to annealing of the acceptor-type defects (presumably zinc vacancies, V_{Zn}) created in the annealing process.

EXPERIMENTAL

Radioactive ion-beams of ^{119}In^{+} were produced at the ISOLDE facility at CERN by proton-induced fission in an UC_x target, element selective laser ionization, and acceleration to 50 keV. Beam intensities of ~3 × 10^{8} ^{119}In/s were obtained. The eMS experiments were carried out in a multi-purpose online implantation chamber,[3] on which an easily detachable module was mounted, which had an

extra vacuum-system together with a Huntington magnetically coupled transporter that facilitated quick removal of samples for offline measurements. In experiments, samples (usually 10 × 10 mm crystals with Ø = 6 mm beamspot) were implanted (for about three times the half-life of the parent in order to build up the activity) and measured simultaneously at temperatures between 300 K and 650 K with halogen lamp heating from behind the sample. The sample was then quickly removed from the beam and vacuum (~10 s) through an exchange volume and dropped into a bath of liquid nitrogen for rapid cooling, after which the offline eMS data were collected with the sample at ~110 K. The time required for cooling of sample and sample holder and mounting in front of the offline detector was about 100 s from implantation temperature T_{imp} = 500 °C and about 30 s from implantation at room temperature based on the analysis of video material during operations. A schematic of the setup used for these measurements is shown in Fig. 1.

The sample is first implanted and measured in an implantation chamber (A) and held at the implantation/measurement temperature by heating from the behind by a halogen lamp. The online spectrum is measured with a Parallel Plate Avalanche Detector (PPAD)[10,11] equipped with a $Ca^{119}SnO_3$ electrode mounted outside the implantation chamber on a conventional drive system. The radiation passes through a few mm of Be foils to filter electrons from the β^- decay of $^{57}Mn/^{119}In$. The sample mounted on a metal holder is subsequently quickly moved from a sample exchanger and dropped into a liquid nitrogen bath (B). After the temperature has stabilized, the sample is moved in position for offline measurements. θ_I and θ_E stand for the implantation angle and emission (measuring) angle, respectively.

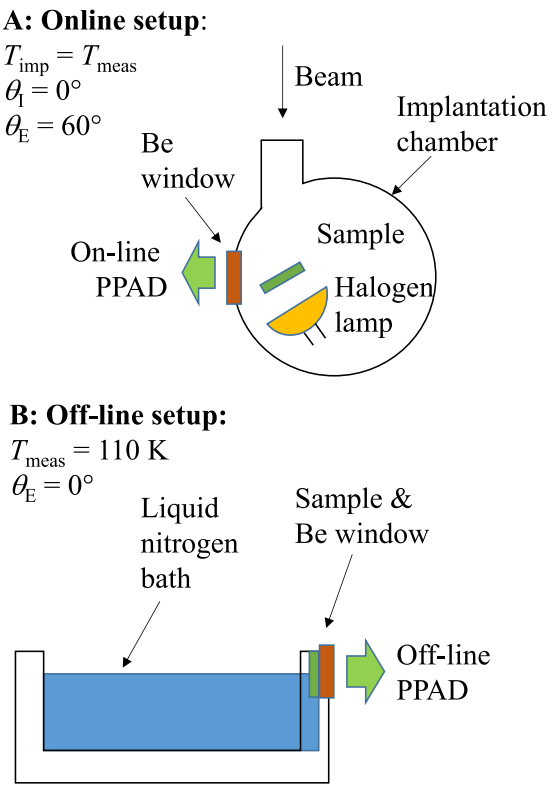

FIG. 1. Schematic diagram of the experimental setup for online experiments (A) and for offline measurements of rapidly cooled implanted samples (B).

In the measurements presented here, the online measurements were carried out with implantations at an angle of θ_I = 30° relative to the sample normal, and the eMS spectra were measured with a resonance detector at 60° relative to the sample normal. In the offline setup, the sample is not fully immersed in liquid nitrogen, but its temperature stabilizes at ~110 K during the measurement. The offline measurements presented here were performed at an emission angle of $\theta_E = 0°$ using a PPAD equipped with a $Ca^{119}SnO_3$ electrode. The maximum fluence was estimated to be $<2 \times 10^{12}$ $^{119}In/cm^2$. Isomer-shifts and velocities are given relative to the center of the spectrum of SnO_2 at room temperature. All eMS spectra have been analyzed using the Vinda analysis code.[12]

THEORY

One of the parameters of importance in eMS is the Debye–Waller factor, also called f-factor. It is related to the vibrational dynamics of the crystal lattice and expresses the probability of recoil-free emission of γ-quanta. It is the same as the so-called B factor (or the temperature factor) in x-ray/neutron scattering experiments. In the Debye approximation, it can be written as[5]

$$f(T,\theta_D) = \exp\left[\frac{-3E_\gamma^2}{k_B\theta_D c^2}\left\{\frac{1}{4} + \left(\frac{T}{\theta_D}\right)^2 \int_0^{\theta_D/T} \frac{x}{e^x - 1}dx\right\}\right], \quad (1)$$

where E_γ is the energy of the γ-quanta (23.9 keV in the case of ^{119}Sn), k_B is the Boltzmann constant, θ_D is the Debye temperature, and c is the speed of light. In Mössbauer spectroscopy, it is convenient to represent lattice sites with different vibrational properties in terms of the Debye temperature of the specific site. It should be mentioned that the Debye temperature is essentially a macroscopic quantity based on the assumption of the shape of the density of state distribution. Different techniques probe the density of state distribution in different ways, and this can result in different findings depending on the experimental technique.[13]

The f-factor decreases with temperature (cf. Fig. 2), making it difficult to accurately determine spectral components with low Debye temperatures at elevated temperatures.

The Debye temperature of substitutional impurities, θ_{eff}, can often be adequately determined from the mass-defect approximation, $\theta_{eff} = \theta_{D,H}\sqrt{M/M_{Fe}}$,[14] where $\theta_{D,H}$ is the Debye temperature of the host lattice and M and M_{Fe} are the masses of the host and Fe atoms, respectively. The Debye temperature of interstitial impurities is usually much lower[15] than that of substitutional impurities.

The resonance area of a spectral component (labeled with i) in emission Mössbauer spectroscopy can be written as

$$A_i(T) = A_0 \cdot p_i(T) \cdot f(T,\theta_{D,i}), \quad (2)$$

where A_0 is a constant depending on the efficiency of the detector and p_i is the site population of the i th spectral component. A_0 is determined by measuring a reference standard. Usually, one applies the restriction $\sum_i p_i(T) = 1$, i.e., no missing components, and

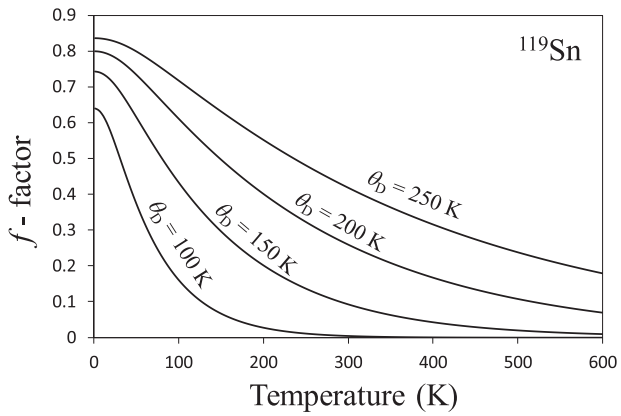

FIG. 2. f-factor for ^{119}Sn as a function of temperature for the Debye temperatures indicated.

solves Eq. (2) for the Debye temperatures. This method works perfectly if there is only one spectral component. Moreover, it can work for more than one component if there are major changes in their spectral areas within the temperature series.

Assuming that the site populations depend only on the implantation temperature, it is possible to estimate the Debye temperatures of spectral components in a different way and re-write Eq. (2) to cancel out the site population for spectra obtained at the online implantation temperature (T_I) and measurement temperature (T_m). Defining $a_i(T) = A_i(T)/A_0$, one obtains

$$\frac{a_i(T_m)}{a_i(T_I)} = \frac{f(T_m, \theta_{D,i})}{f(T_I, \theta_{D,i})}. \quad (3)$$

Figure 3 shows the calculated curves of $a_i(T_m)/a_i(T_I)$ as a function of implantation temperature for different Debye temperatures and for measurement temperature T_m = 110 K.

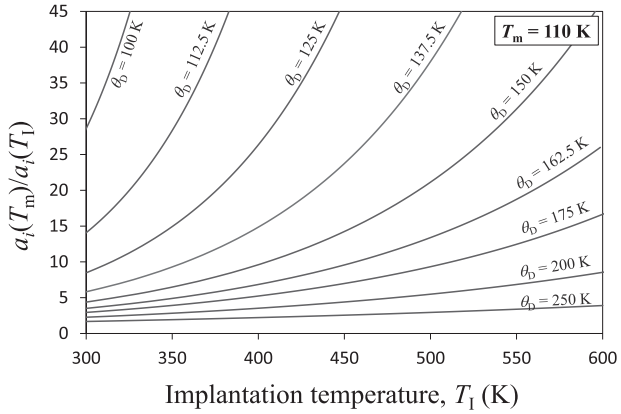

FIG. 3. Calculated curves of the $a_i(T_m)/a_i(T_I)$ ratio as a function of implantation temperature for different Debye temperatures and at measurement temperature T_m = 110 K.

The $a_i(T_m)/a_i(T_I)$ area ratio increases with implantation temperature and is steepest for spectral components with low Debye temperatures.

RESULTS

The spectra obtained in this study are shown in Fig. 4. The dominating feature of all spectra is a single line assigned to Sn^{4+} at $v \approx 0$ mm/s, while a line due to Sn^{2+} is observed at $v \approx -2.5$ mm/s. Generally, the results are similar to those obtained by Mølholt *et al.*[6]

The Sn^{2+} line is more intense in the spectra obtained at T_m = 110 K (right side of Figs. 4 and 5), implying that the Debye temperature of the Sn^{2+} line is lower than that of the Sn^{4+} line, in accordance with results from similar systems.[16,17]

The samples used in this study were pre-implanted with ~10^{11} ^{119}In/cm^2 to avoid possible dose dependence effects.[6] Neither time-dependence nor dose-dependence of the results was observed, so the assumption that the site population depends only on the implantation temperature is most likely fulfilled. Consequently, applying Eq. (3), a diagram similar to Fig. 3 can be employed to determine Debye temperatures (see Fig. 6).

The data obtained for Sn^{4+} follow a simple trend, consistent with a Debye temperature of θ_D = 239(3) K. The data obtained for Sn^{2+} show a more complicated behavior. For temperatures $T_I \leq 577$ K, the data indicate a Debye temperature of θ_D = 180(5) K (or even lower at room temperature), while the point obtained at 646 K indicates a Debye temperature of θ_D = 210(10) K. This sudden increase in the Debye temperature of the Sn^{2+} line reveals a change in the nature of the Sn^{2+} spectral line. This coincides with the temperature at which the relative intensity of the Sn^{2+} line starts to increase (see Fig. 5), and supports the conclusion that the Sn^{2+} component

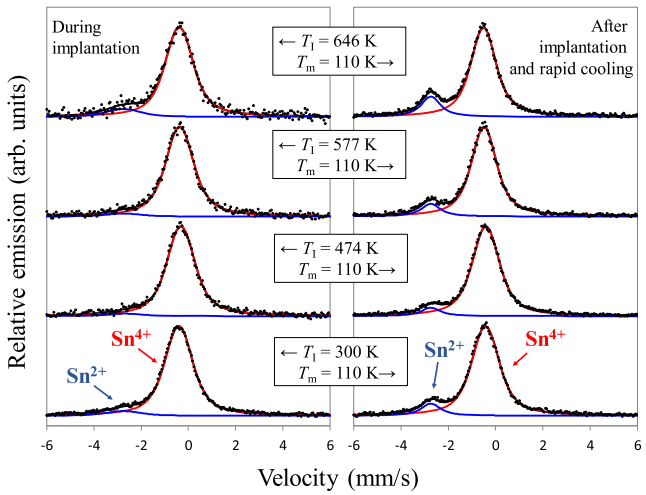

FIG. 4. Left: ^{119}Sn eMS spectra obtained after implantation of ^{119}In into a ZnO sample held at the implantation temperature (T_I). Right: The spectra obtained after rapid cooling of the samples and measurements at T_m = 110 K during the decaying activity.

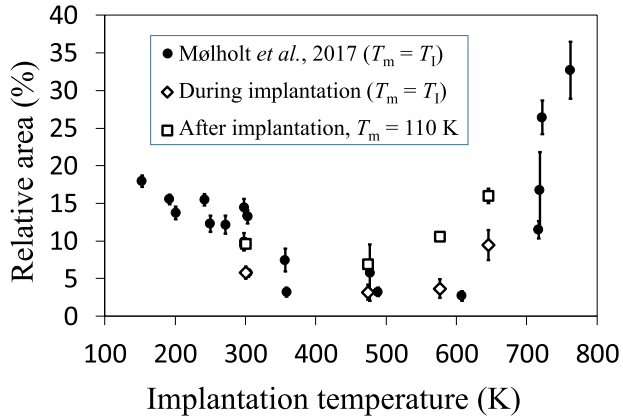

FIG. 5. Relative area of the Sn^{2+} line. Filled dots: Data from Mølholt *et al.*[6] Open symbols: This work. The diamonds show the spectral area obtained in spectra where the measurement temperature, T_m, is the same as the implantation temperature, T_I. The squares show the relative area obtained in spectra of rapidly cooled samples at T_m = 110 K, after implantation at the temperature indicated.

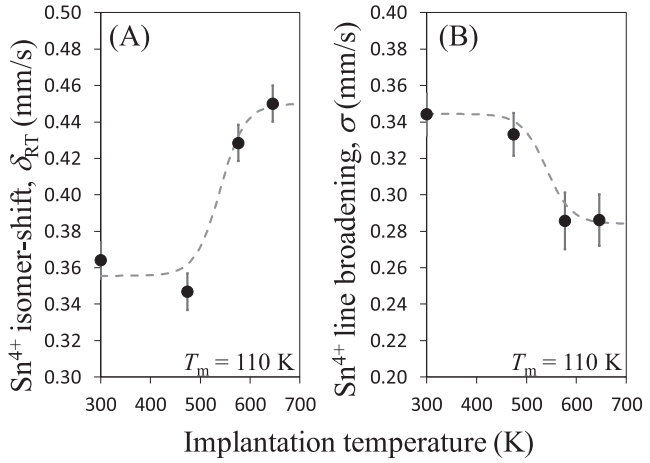

FIG. 7. Isomer-shift (A) and line broadening (B) of the Sn^{4+} line obtained from the analysis of the spectra of rapidly cooled samples (Fig. 4). The dashed lines are a guide to the eye.

observed at $T < 400$ K differs from the Sn^{2+} component observed at higher temperatures.

The fact that the offline spectra are measured at the same temperature allows studying the effect of implantation/annealing temperature on the spectra without making assumptions on whether the line position follows the second-order Doppler shift or whether linewidths are temperature dependent.

The isomer-shift and linewidth of the Sn^{4+} component in the rapidly cooled spectra obtained at T_m = 110 K are shown in Fig. 7. Both parameters show a change in the Sn^{4+} line at around 550 K. The apparent narrowing of the spectral line indicates a more regular environment or crystalline lattice site, consistent with the annealing of implantation damage.

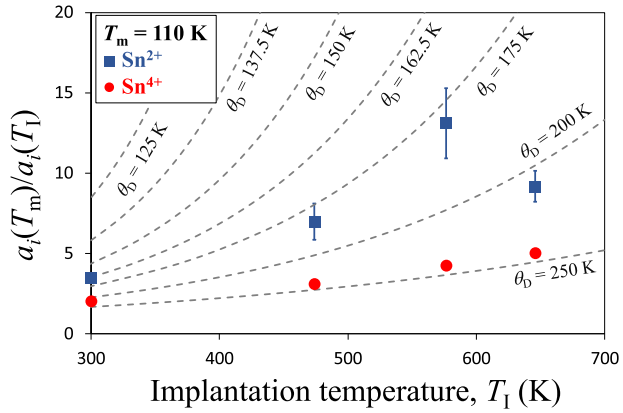

FIG. 6. $a_i(T_m)/a_i(T_I)$ vs implantation temperature data obtained from the analysis of the data in Fig. 4 along with theoretical curves for different Debye temperatures (Fig. 3).

DISCUSSION

The data presented here enable the identification of three annealing transitions for Sn implanted in ZnO. The first is a broad annealing stage at $T \leq 400$ K, where the majority of Sn^{2+} is converted into Sn^{4+} (see Fig. 5). This is similar to the annealing of the spectral component assigned to Fe^{2+} in local amorphous regions due to the implantation damage observed in similar experiments utilizing ^{57}Mn implanted ZnO.[18]

The second annealing stage sets in at $T \approx 550$ K, as reflected by the narrowing and the shift of the Sn^{4+} line (see Fig. 7). There is no significant change in the area ratio between Sn^{2+} and Sn^{4+} at this stage, so it is unlikely to be due to annealing of electrically active defects, which would be expected to affect the relative ratio of the two components. The narrowing of the spectral line suggests annealing of some structural defects, resulting in a change of the Sn^{4+} site to a more regular lattice site. It has been found that the isomer-shift of Sn^{4+} decreases with increased application of external pressure,[19,20] which suggests that the increase in isomer-shift observed here [Fig. 7(a)] is due to a relaxation of strain in the vicinity of the probe, which may be attributed to recombination of Frenkel pairs in the vicinity of the probe atom.

The third annealing stage is observed at $T \geq 600$ K, where the relative intensity of the Sn^{2+} line increases (left side of Fig. 4). Mølholt *et al.*[6] attributed this stage to annealing of acceptor defects created in the annealing process. In the present work, it has been possible to determine, additionally, that the Debye temperature of Sn^{2+} below the third annealing stage is lower than the Debye temperature of Sn^{2+} formed at this annealing stage (cf. Fig. 6). This is similar to the results obtained by Weyer *et al.*[21] in their eMS studies of the amorphous to crystalline transition in silicon. These authors observed a lowering of the average Debye temperature (increased intensity of components with low Debye temperatures) upon amorphization of silicon by ion implantation.

Tuomisto *et al.*[22] employed positron annihilation spectroscopy of electron-irradiated ZnO and reported an annealing stage at about

550 K consisting of the recovery of both O vacancies and (the remaining) Zn vacancies. While Zn vacancies are candidates that could give rise to the acceptor defects needed for stabilizing the Sn^{4+} state, the annealing of the O vacancies can be related to the structural relaxation observed in the present study at around 550 K.

A potential candidate for the study of the Debye temperatures at probe sites with annealing is the recently reported Sn-vacancy complex in diamond,[23] where it is speculated that upon room temperature implantation, Sn-vacancy complexes and C vacancies are created, which after annealing restructure to the SnV center with Sn on unperturbed bond center sites. Theoretical studies of In implanted diamond also show the formation of the stable V_C-In-V_C structure with In in the BC site preceded by the formation of two C atoms in interstitial positions.[24]

Given the sensitivity of the Mössbauer isomer-shift to the charge density in the immediate vicinity of the probe, our system combining low temperature eMS with annealing studies should allow the tracking of the development of the SnV centers following implantation of Sn probes in diamond and related substrates with potential applications in nanophotonics and quantum communications.

While our emphasis has been on the application of the new equipment for determination of local Debye temperatures at probe sites, all experimental methods that require parent isotopes with lifetime of minutes for sample manipulation that cannot be performed inside an evacuated implantation chamber can benefit from this new equipment. This includes all types of chemistry where implantation into easily dissolved substrates can be used to perform radiochemistry using ^{119}In or ^{57}Mn for eMS or ^{68}Cu for Perturbed Angular Correlation (PAC) measurements.[25]

CONCLUSIONS

An apparatus and a method to perform offline emission Mössbauer spectroscopy measurements of samples immediately after implantation of short-lived parents (on timescales of minutes) have been developed. It has been demonstrated that this setup allows accurate determination of Debye temperatures of spectral components if certain criteria are fulfilled.

In the case of ^{119}In-implanted ZnO, three annealing stages could be identified by analyzing the Debye temperatures. The results reveal that Sn^{2+} observed at $T < 600$ K has a lower Debye temperature than Sn^{2+} observed at $T > 600$ K. The former can be related to Sn^{2+} in damaged local regions, and the latter can be related to Sn^{2+} on regular lattice sites at $T > 600$ K. An intermediate annealing stage is observed at ~550 K, related to structural relaxation of the lattice by the annihilation of Frenkel pairs.

ACKNOWLEDGMENTS

We acknowledge the support of the ISOLDE collaboration and technical teams. Fruitful discussion with Professor D. C. Lupascu University of Duisburg-Essen is acknowledged. I.U. acknowledges the support of the Ministry of Economy and Competitiveness (MINECO/FEDER) under Project No. RTI2018-094683-B-C55 and Basque Government Grant No. IT-1005-16. K.B.R., H.M., and D.N. acknowledge the support of Department of Science and Innovation (South Africa). B.Q., S.Ó., and H.P.G. acknowledge support from the University of Iceland Research Fund. J. G. Martins Correia is acknowledged for technical assistance during the beam time. The Federal Ministry of Education and Research (BMBF) through Grant Nos. 05K16PGA, 05K16SI1, and 05K19SI1 "eMMA" is acknowledged. The European Commission through the Horizon 2020 programme (Grant Nos. 654002 and ENSAR 2) is acknowledged.

DATA AVAILABILITY

The data that support the findings of this study are available from the corresponding author upon reasonable request.

REFERENCES

[1]C. W. White, C. J. McHargue, P. S. Sklad, L. A. Boatner, and G. C. Farlow, "Ion implantation and annealing of crystalline oxides," Mater. Sci. Rep. **4**, 41–146 (1989).
[2]See http://e-ms.web.cern.ch/ for The Mössbauer collaboration at ISOLDE/CERN; retrieved 1 June 2020.
[3]K. Johnston, J. Schell, J. G. Correia, M. Deicher, H. P. Gunnlaugsson, A. S. Fenta, E. David-Bosne, A. R. G. Costa, and D. C. Lupascu, "The solid state physics programme at ISOLDE: Recent developments and perspectives," J. Phys. G: Nucl. Part. Phys. **44**, 104001 (2017).
[4]G. Weyer, "Mössbauer spectroscopy at ISOLDE," Hyperfine Interact. **129**, 371–390 (2000).
[5]P. Gütlich, E. Bill, and A. X. Trautwein, *Mössbauer Spectroscopy and Transition Metal Chemistry: Fundamentals and Applications* (Springer-Verlag Berlin and Heidelberg, 2011).
[6]T. E. Mølholt, H. P. Gunnlaugsson, K. Johnston, R. Mantovan, J. Röder, V. Adoons, A. M. Gerami, H. Masenda, Y. A. Matveyev, M. Ncube, I. Unzueta, K. Bharuth-Ram, H. P. Gislason, P. Krastev, G. Langouche, D. Naidoo, S. Ólafsson, A. Zenkevich, and ISOLDE Collaboration, "Charge states and lattice sites of dilute implanted Sn in ZnO," J. Phys.: Condens. Matter **29**, 155701 (2017).
[7]H. P. Gunnlaugsson, R. Mantovan, H. Masenda, T. E. Mølholt, K. Johnston, K. Bharuth-Ram, H. Gíslason, G. Langouche, D. Naidoo, S. Ólafsson, A. Svane, G. Weyer, and the ISOLDE Collaboration, "Defect annealing in Mn/Fe implanted TiO_2 (rutile)," J. Phys. D: Appl. Phys. **47**, 065501 (2014).
[8]G. Weyer, S. Damgaard, J. W. Petersen, and J. Heinemeier, "Mössbauer study of ^{119}Sn defects in silicon from ion implantations of radioactive ^{119}In," Hyperfine Interact. **7**, 449–453 (1979).
[9]G. Weyer, S. Damgaard, J. W. Petersen, and J. Heinemeier, "Sn impurity defects in germanium from ion implantations of radioactive ^{119}In," Phys. Lett. A **76**, 321–323 (1980).
[10]G. Weyer, "Applications of parallel-plate avalance counters in Mössbauer spectroscopy," in *Mössbauer Effect Methodology*, edited by I. J. Gruverman and C. W. Seidel (Springer, Boston, MA, 1976).
[11]G. Weyer, "Mössbauer resonance-scattering techniques for emission spectroscopy on gamma radiation from short-lived radioactive isotopes," Nucl. Instrum. Methods Phys. Res. **186**, 201–209 (1981).
[12]H. P. Gunnlaugsson, "Spreadsheet based analysis of Mössbauer spectra," Hyperfine Interact. **237**, 79 (2016).
[13]Y. Kagan and Y. A. Iosilevskii, "The Mössbauer effect for an impurity nucleus in a crystal.I," Sov. Phys. JETP **15**, 182 (1962).
[14]Y.-L. Chen and D.-P. Yang, *Mössbauer Effect in Lattice Dynamics: Experimental Techniques and Applications* (John Wiley & Sons, 2007).
[15]G. Weyer, A. Burchard, M. Fanciulli, V. N. Fedoseyev, H. P. Gunnlaugsson, V. I. Mishin, R. Sielemann, and The ISOLDE Collaboration, "The electronic configuration of substitutional Fe in silicon," Physica B **273-274**, 363–366 (1999).
[16]K. F. E. Williams, C. E. Johnson, J. Greengrass, B. P. Tilley, D. Gelder, and J. A. Johnson, "Tin oxidation state, depth profiles of Sn^{2+} and Sn^{4+} and oxygen diffusivity in float glass by Mössbauer spectroscopy," J. Non-Cryst. Solids **211**, 164–172 (1997).

[17]R. Mantovan, S. Spiga, and M. Fanciulli, "Low temperature CEMS of Sn-implanted SiO_2," Hyperfine Interact. **165**, 69–73 (2005).
[18]H. P. Gunnlaugsson, K. Bharuth-Ram, K. Johnston, G. Langouche, R. Mantovan, T. E. Mølholt, D. Naidoo, O. Ólafsson, and G. Weyer, "Damage annealing in low temperature Fe/Mn implanted ZnO," Hyperfine Interact. **230**, 175–180 (2015).
[19]H. S. Möller, "Pressure dependence of the isomer shift of Sn^{119}," Z. Phys. A **212**, 107–121 (1968).
[20]E. V. Kapitanov and E. N. Yakovlev, "Mössbauer investigation of SnO under hydrostatic pressure up to 41 kbar," Phys. Status Solidi A **51**, 641–644 (1979).
[21]G. Weyer, S. Damgaard, J. Petersen, and J. Heinemeier, "Comparison of impurity defect structures formed by ion implantations in amorphous and crystalline silicon," Nucl. Instrum. Methods Phys. Res. **199**, 441–444 (1982).
[22]F. Tuomisto, K. Saarinen, D. C. Look, and G. C. Farlow, "Introduction and recovery of point defects in electron-irradiated ZnO," Phys. Rev. B **72**, 085206 (2005).
[23]U. Wahl, J. G. Correia, R. Villareal, E. Bourgeois, M. Gulka, M. Nesladek, A. Vantomme, and L. M. V. Pereira, "Direct structural indentification of the split-vacany configuration for implanted Sn in diamond," Phys. Rev. Lett. **125**, 045301 (2020).
[24]B. P. Doyle, J. K. Dewhurst, J. E. Lowther, and K. Bharuth-Ram, "Lattice locations of indium implanted in diamond," Phys. Rev. B **57**, 4965 (1998).
[25]A. S. Fenta, S. Pallada, J. G. Correia, M. Stachura, K. Johnston, A. Gottberg, A. Mokhles Gerami, J. Röder, H. Grawe, B. A. Brown, U. Köster, T. M. Mendonça, J. P. Ramos, B. A. Marsh, T. Day Goodacre, V. S. Amaral, L. M. C. Pereira, M. J. G. Borge, and H. Haas, "The ^{68m}Cu/^{68}Cu isotope as a new probe for hyperfine studies: The nuclear moments," Europhys. Lett. **115**, 62002 (2016).